



Deciphering microbial responses to H₂S inhibition of typical functional microorganisms in anaerobic digestion ecosystems

Title	Deciphering microbial responses to H ₂ S inhibition of typical functional microorganisms in anaerobic digestion ecosystems
Author(s)	Shu, Wenhui; Du, Bang; Wu, Guangxue
Publication Date	2025-04-21
Publisher	Elsevier
Repository DOI	https://doi.org/10.1016/j.cej.2025.162766



Deciphering microbial responses to H₂S inhibition of typical functional microorganisms in anaerobic digestion ecosystems

Wenhui Shu, Bang Du , Guangxue Wu* 

Civil Engineering, School of Engineering, College of Science and Engineering, University of Galway, Galway H91 TK33, Ireland

ARTICLE INFO

Keywords:

H₂S inhibition
Sulfate-reducing bacteria
Methanogens
Detoxification

ABSTRACT

Hydrogen sulfide (H₂S), a product of sulfate reduction in anaerobic digestion (AD) systems, poses severe challenges by reducing methane production and destabilizing system performance. Despite extensive studies on H₂S toxicity, the specific responses and adaptation mechanisms to H₂S stress of key functional microorganisms in AD systems remain insufficiently elucidated. Four reactors were operated with sequencing batch reactor (SBR) and continuous flow reactor (CFR) configurations under varying COD/sulfate ratios (2 and 1) to investigate microbial response to H₂S inhibition. Long-term experiments demonstrated that CFRs combined with a COD/sulfate ratio of 1 achieved superior sulfate reduction and ethanol degradation rates under H₂S stress, while SBRs with a COD/sulfate ratio of 2 facilitated methanogenic activity. Batch inhibition experiments revealed that ethanol-oxidizing bacteria (EOB) and incomplete oxidizing sulfate-reducing bacteria (IO-SRB) exhibited greater H₂S tolerance in CFRs, with EOB (IC₅₀ = 51.2–185.1 mg/L) generally outperforming IO-SRB (IC₅₀ = 47.4–97.7 mg/L). While acetoclastic methanogens (AM) and complete oxidizing sulfate-reducing bacteria showed enhanced H₂S tolerance in SBRs compared to CFRs, particularly AM in SBR with the COD/sulfate ratio of 2 (IC₅₀ = 113.2 mg/L). Microbial adaptation analysis demonstrated that SBRs promoted *Methanothrix* enrichment, enhancing detoxification capacity by specifically increasing the relative abundance of genes encoding thiosulfate sulfurtransferase to mitigate H₂S toxicity. *Desulfomicrobium* and *Geobacter* were significantly enriched in CFRs, and they mitigated H₂S inhibition through increased cytochrome *bd* oxidase and cysteine synthase genes, respectively. Furthermore, thioredoxin and cysteine desulfurase protein repair genes sustained microbial metabolism under H₂S stress. This study provides critical insights into microbial tolerance and adaptive strategies to H₂S under different reactor configurations, offering guidance for optimizing AD processes in sulfate-rich wastewater treatment.

1. Introduction

Anaerobic digestion (AD) is a widely used technology for wastewater treatment and renewable energy generation. By converting organic matter into methane and carbon dioxide through microbial processes, AD offers both environmental and economic benefits, making it an attractive option for treating industrial and municipal wastewater [1,2]. However, the presence of sulfate in wastewater, commonly originating from industries such as paper manufacturing, pharmaceuticals, and food processing, can pose a dual challenge to AD systems [3,4]. Specifically, sulfate-reducing bacteria (SRB) are categorized into incomplete oxidizing SRB (IO-SRB) and complete oxidizing SRB (CO-SRB), where IO-SRB oxidize substrates to acetate and compete with acetogenic bacteria, while CO-SRB compete with methanogens for key substrates, such as acetate, and activities of both SRB can generate toxic hydrogen sulfide

(H₂S) [5,6]. H₂S diffuses readily through microbial membranes, disrupting cellular respiration and interfering with key enzymatic processes [7]. At elevated concentrations, H₂S targets disulfide bond and metalloproteins, leading to oxidative stress, enzyme inactivation, and potential system failure [8]. Consequently, H₂S accumulation can substantially impair the performance of AD systems, particularly by inhibiting methanogenic activity [9,10]. For example, the inhibitory concentration of H₂S for methanogens has been reported to range from 50 to 400 mg/L under different environmental conditions [11,12]. Therefore, understanding microbial responses and adaptation mechanisms under H₂S-stressed conditions is critical for enhancing the performance and resilience of AD processes in sulfate-rich wastewater treatment systems.

While H₂S is known to inhibit anaerobic digestion, microbial responses to H₂S stress vary among different microbial groups [13,14,15].

* Corresponding author.

E-mail address: guangxue.wu@universityofgalway.ie (G. Wu).

<https://doi.org/10.1016/j.cej.2025.162766>

Received 24 February 2025; Received in revised form 10 April 2025; Accepted 16 April 2025

Available online 18 April 2025

1385-8947/© 2025 The Authors. Published by Elsevier B.V. This is an open access article under the CC BY license (<http://creativecommons.org/licenses/by/4.0/>).

These differences in tolerance and metabolic responses are observed across various trophic levels, including syntrophic bacteria, SRB, and methanogens, ultimately threatening the overall stability and efficiency of AD systems [16]. Syntrophic bacteria have been reported to be less susceptible to sulfide inhibition than methanogens, with toxicity thresholds comparable to those of SRB [17]. SRB, such as *Desulfovibrio* and *Desulfomicrobium*, display diverse responses to H₂S, depending on their growth kinetics and ability to maintain metabolic activity under high sulfide concentrations [18]. Several studies have systematically compared the sulfide tolerance between IO-SRB and CO-SRB. For instance, Icgem and Harrison [19] evaluated SRB dynamics under acetate-fed anaerobic continuous bioreactors and found that sulfide exposure suppressed *Desulfonema* (CO-SRB) and *Desulfobulbus* (IO-SRB), while *Desulfobacter* and *Desulfococcus* (CO-SRB), as well as *Desulfovibrionaceae* (IO-SRB) showed higher tolerance and maintained abundant at elevated sulfide loadings. Similarly, methanogens also exhibit varying degrees of tolerance to H₂S. Hydrogenotrophic methanogens (HM) show higher resilience to H₂S inhibition, which is attributed to their streamlined metabolic processes and enhanced ability to utilize hydrogen as an electron donor, while acetoclastic methanogens (AM) are more susceptible to H₂S toxicity, likely due to their reliance on acetate metabolism and limited stress response pathways [20,21,22].

Although the inhibitory effects of H₂S on individual functional microorganisms have been widely studied, limited attention has been paid to how reactor operational modes influence microbial responses under H₂S stress. Given that operational mode determines the temporal and spatial distribution of H₂S, it can substantially affect microbial exposure and shape community assembly [23,24]. Sequencing batch reactors (SBRs) operate in cyclic feeding and discharge modes, resulting in fluctuating H₂S concentrations. These dynamic conditions may favor fast-growing microorganisms or those that are capable of rapid recovery during low stress conditions [6,25]. Conversely, continuous flow reactors (CFRs) maintain steady-state conditions, exposing microbial communities to consistent H₂S levels. This stable environment may promote the enrichment of H₂S-tolerant species with slower growth rates but greater resilience [18,26,27]. The differences in microbial adaptation and performance between SBRs and CFRs have important implications for optimizing AD processes under H₂S-stressed conditions. However, limited studies have been conducted in this field.

Furthermore, exploring microbial detoxification and adaptation mechanisms is essential to address the multifaceted challenges posed by H₂S inhibition. Microorganisms counteract H₂S toxicity through a range of strategies [28,29]. For instance, rhodanese enzymes, such as thio-sulfate sulfurtransferase (TST), play a pivotal role in transforming H₂S into less toxic sulfur species, thereby reducing cellular damage [30,31]. This enzyme is highly conserved across species and has been shown to effectively mitigate H₂S toxicity in various organisms. Interestingly, some prokaryotes exhibit unique mechanisms to resist H₂S toxicity by utilizing alternative terminal oxidases, such as the structural simplicity bd-type quinol oxidases [32]. Moreover, enzymes involved in oxidative stress defense and protein repair provide additional protection, enabling microorganisms to sustain metabolic activity under H₂S-induced stress [33,34]. However, genetic and molecular studies on H₂S tolerance have predominantly focused on model organisms such as *Escherichia coli*, *Acinetobacter baumannii*, *Bacillus subtilis*, and *Staphylococcus aureus*, with limited research on key microorganisms in AD systems.

This study aimed to unravel the complex dynamics of microbial communities and their functional adaptations under H₂S stress in AD systems treating sulfate-rich wastewater, employing two distinct reactor configurations (i.e., SBRs and CFRs) with COD/sulfate ratios of 2 and 1. The specific objectives were to: (1) evaluate the impacts of H₂S inhibition on key metabolic processes, including sulfate reduction, ethanol degradation, acetate degradation, and methane production; (2) analyze the adaptation and dynamic changes of microbial communities under different reactor operational modes; and (3) elucidate the metabolic regulation and detoxification mechanisms employed by functional

microorganisms under H₂S stress. The outcomes of this study can help bridge knowledge gaps regarding microbial community responses and system performance under H₂S stress, providing fundamental support for optimizing anaerobic treatment technologies for treating sulfate-rich wastewater.

2. Materials and methods

2.1. Experimental setup and operational conditions

Four 5 L effective volume reactors (two SBRs and two CFRs) were operated with COD/sulfate ratios of 2 and 1, designated as SBR_{C/S=2}, SBR_{C/S=1}, CFR_{C/S=2}, and CFR_{C/S=1}, respectively. All reactors were fed with the same sulfate concentration to ensure consistent inhibitory conditions caused by H₂S as the metabolic product. The inoculum was collected from lab-scale anaerobic ethanol-fed reactors. Each reactor was designed with a suspended solids (SS) concentration of 6.4 ± 0.2 g/L and a volatile suspended solids (VSS) concentration of 4.5 ± 0.3 g/L. The reactors were maintained at 35 °C with a hydraulic retention time of 48 h and a solids retention time of 25 d. The typical operation cycle in SBRs included a 23 h anaerobic reaction phase comprising an initial 10 min rapid feeding of 2.5 L of synthetic wastewater, followed by 50 min of settling and 10 min discharge of 2.5 L of supernatant. In CFRs, 2.5 L of synthetic wastewater was fed continuously over a 23 h period with mixing, followed by 50 min settling and 10 min discharge of 2.5 L of supernatant.

The synthetic wastewater contained 2500 mg/L of sulfate (3698 mg/L Na₂SO₄). Ethanol was used as the carbon source, with concentrations of 5000 mg COD/L in SBR_{C/S=2} and CFR_{C/S=2}, and 2500 mg COD/L in SBR_{C/S=1} and CFR_{C/S=1}. The inorganic salt solution included 191 mg/L NH₄Cl, 46 mg/L Na₂HPO₄, 200 mg/L CaCl₂·6H₂O, 200 mg/L MgCl₂, 5000 mg/L KHCO₃ in SBR_{C/S=2} and CFR_{C/S=2} and 2500 mg/L KHCO₃ in SBR_{C/S=1} and CFR_{C/S=1}, along with 1 mL/L of trace elements. The trace elements contained 1000 mg/L FeCl₂·4H₂O, 100 mg/L CoCl₂·H₂O, 200 mg/L NiCl₂·6H₂O, 100 mg/L MnCl₂·4H₂O, 100 mg/L Na₂MoO₄·2H₂O, 100 mg/L H₃BO₃, 100 mg/L Na₂WO₄·2H₂O, and 100 mg/L Na₂SeO₃ [35].

2.2. Batch experiments

2.2.1. Cycle experiments

Under steady state conditions, cycle experiments were conducted using 160 mL serum bottles with a working volume of 100 mL and a headspace of 60 mL. Each bottle was filled with 50 mL of synthetic wastewater and 50 mL of sludge collected from each reactor. Key parameters, including ethanol degradation, volatile fatty acids (VFAs) production and consumption, methane production, sulfate reduction, and sulfide generation, were monitored over a 24 h cycle.

2.2.2. Inhibition experiments

To evaluate the impact of H₂S inhibition on microbial metabolism in the four reactors, batch experiments were conducted using three different substrate sources: ethanol, acetate, and H₂/CO₂. Initial sulfide concentrations were set at 0, 200, 400, 800, 1600, and 3200 mg/L. A sulfide stock solution of 30000 mg S/L was prepared by dissolving Na₂S·9H₂O in nitrogen purged ultrapure water, and the sludge from each reactor was washed three times with inorganic salt solution to eliminate residual sulfide.

For the ethanol-based batch inhibition experiments, synthetic wastewater containing 1000 mg COD/L of ethanol and 500 mg/L sulfate was prepared. Each serum bottle, with a 100 mL working volume, was filled with washed sludge, synthetic wastewater, and sulfide stock solution to achieve an initial biomass concentration of 2 g VSS/L and the desired sulfide concentration. In acetate-based batch inhibition experiments, 1000 mg COD/L of acetate was used as the sole organic carbon source, with all other conditions remaining the same as in the ethanol-

based experiments. The serum bottles were then purged with nitrogen gas to ensure anaerobic conditions and sealed with butyl rubber stopper and aluminum crimp seals. For the H₂/CO₂-based batch inhibition experiments, serum bottles were purged with a gas mixture of H₂/CO₂ (v/v = 80/20) and pressurized to 1000 hPa before sealing.

The initial pH of all serum bottles was adjusted to 8.0 using 0.2 M HCl or 0.2 M NaOH solutions [36]. All sealed bottles were incubated in an air-shaking incubator at 35 °C and 170 rpm, with periodic sampling to monitor metabolic activity. Each experiment was performed in triplicate.

2.3. Analytical methods

SS and VSS concentrations were determined using standard methods [37]. Ethanol and VFAs were quantified using a gas chromatograph (8860, Agilent Technologies, USA) equipped with a flame ionization detector. Sulfate was analyzed using a nutrient analyzer (Gallery Plus, Thermo Fisher Scientific, USA). Total dissolved sulfide (TDS) in solution was determined using the methylene blue method [37]. pH was measured using a Hach portable meter (HQ40D, Hach, USA). The H₂S concentration was calculated using the following equation [36]:

$$[H_2S] = \frac{[TDS]}{1 + \frac{K}{10^{-pH}}} \quad (1)$$

where $[H_2S]$ is the H₂S concentration in the aqueous phase (mg/L), $[TDS]$ is the total dissolved sulfide concentration (mg/L), and K is the first-step ionization equilibrium constant of H₂S, with a value of $10^{-6.83}$ at 35 °C.

Biogas composition was measured using a gas chromatograph (7890A, Agilent Technologies, USA) with a thermal conductivity detector. The modified Gompertz equation was used to model cumulative CH₄ production [38].

$$P = P_{max} \exp \left\{ - \exp \left[\frac{e R_{max}}{P_{max}} (\lambda - t) + 1 \right] \right\} \quad (2)$$

where P is the cumulative CH₄ production (mL/L), P_{max} is the maximum CH₄ production potential (mL/L), R_{max} is the maximum CH₄ production rate (mL/(L·h)), λ is the CH₄ production lag phase (h), t is the reaction time (h), and e is 2.71828.

2.4. Inhibition model

H₂S inhibition on microbial metabolism was characterized as a non-competitive process, where the inhibitory effect is independent of substrate concentration. A modified non-competitive model was employed to describe the inhibition of H₂S on the metabolic activity of functional microbial groups [39].

$$I(\%) = 100 \times \left(1 - \frac{1}{1 + \left(\frac{[H_2S]}{a} \right)^b} \right) \quad (3)$$

$$I(\%) = \frac{R_{inhibited}}{R_{controlled}} \times 100 \quad (4)$$

where $I(\%)$ is the inhibition response, a is the half-maximal inhibitory concentration (IC₅₀, mg/L) of H₂S for microbial activity, b is the fitting parameter, $R_{inhibited}$ represents the metabolic activity of the functional microbial community under the desired H₂S concentration in batch inhibition experiments. This activity is characterized by the specific rates such as the ethanol degradation rate for ethanol-oxidizing bacteria (EOB), the sulfate reduction rate for IO-SRB, the sulfate reduction rate for CO-SRB, the acetoclastic methanogenesis rate for AM, the hydrogenotrophic methanogenesis rate for HM, and sulfate reduction rate for hydrogenotrophic SRB (HSRB). $R_{controlled}$ is the metabolic activity of the

microbial community at an H₂S concentration of 0 mg/L.

2.5. Metagenomic analysis

Sludge samples were collected from each reactor under steady-state conditions to analyze microbial community composition and relative abundance of functional genes. DNA was extracted using the DNeasy PowerSoil Pro Kit (QIAGEN, Germany), and its concentration and purity were assessed with a NanoDrop One (Thermo Fisher Scientific, USA). High-throughput sequencing was performed on the Illumina HiSeq 2500 platform (Illumina, San Diego, USA), generating paired-end 150 bp reads. Quality control of the raw reads was performed using the Trimmomatic software (<https://github.com/usadellab/Trimmomatic/>), and the clean reads were subsequently assembled using MEGAHIT (<https://github.com/voutcn/megahit/>). The assembled scaffolds were used for open reading frame (ORF) prediction with MetaGeneMark (<https://github.com/gatech-genemark/MetaGeneMark-2>), and redundancy removal was performed using Mmseqs (<https://github.com/soedinglab/MMseqs2/>) to generate a non-redundant gene catalog (Unigenes). Taxonomic annotations were obtained by aligning the Unigenes against the NCBI-NR database, and functional annotations were performed using the Kyoto Encyclopedia of Genes and Genomes (KEGG) database [40]. Raw sequencing data were deposited to the NCBI BioProject database under the accession number PRJNA1246246.

2.6. Statistical analysis

Statistical analysis was conducted using Microsoft Excel (2021), with a t -test applied to assess differences in a specific parameter between the two experimental groups. A P-value of less than 0.05 was considered indicative of a statistically significant difference.

3. Results and discussion

3.1. System performance

3.1.1. Distinct reactor performances under H₂S stress

Four reactors were operated for a total of 76 days, and Table 1 presents the initial and steady-state conditions of COD, sulfate, SS and VSS concentrations in the reactors. During steady-state operation, while acetate and propionate were occasionally detected in the effluent (Fig. S1), VFAs were generally absent, and complete COD removal was consistently achieved in all reactors. Furthermore, the sulfate concentration in the effluents of SBR_{C/S=2}, SBR_{C/S=1}, CFR_{C/S=2}, and CFR_{C/S=1}

Table 1

Summary of SS, VSS, COD, and sulfate concentrations and/or removal percentages during the long-term operation of the four reactors.

		SBR _{C/S=2}	CFR _{C/S=2}	SBR _{C/S=1}	CFR _{C/S=1}
Influent	COD (mg/L)	5219.8 ± 56.8		2669.6 ± 69.8	
	Sulfate (mg/L)	2734.1 ± 88.5		2748.2 ± 71.2	
	pH	8.2 ± 0.1			
Effluent	COD (mg/L)	Not detected based on the tested VFAs			
	Sulfate (mg/L)	247.5 ± 34.5	162.2 ± 29.1	1149.7 ± 27.0	152.6 ± 49.4
	Sulfate removal percentage (%)	91.0 ± 1.1	94.1 ± 1.0	57.9 ± 2.1	94.4 ± 1.7
	pH	7.8 ± 0.1	7.8 ± 0.1	7.7 ± 0.1	7.8 ± 0.1
					0.1
					0.1
Sludge	Initial SS (g/L)	6.4 ± 0.2			
	Initial VSS (g/L)	4.5 ± 0.3			
	Steady State SS (g/L)	4.3 ± 0.1	3.9 ± 0.1	3.3 ± 0.1	3.2 ± 0.1
	Steady State VSS (g/L)	3.6 ± 0.1	3.1 ± 0.1	2.8 ± 0.1	2.5 ± 0.1
		0.1	0.1		0.1

Note: COD values were estimated by converting ethanol and VFAs concentrations to their theoretical oxygen demand equivalents.

was 247.5 ± 34.5 , 1149.7 ± 27.0 , 162.2 ± 29.1 , and 152.6 ± 49.4 mg/L, respectively, indicating lower sulfate removal efficiency in $SBR_{C/S=1}$. The results showed that SBRs under a COD/sulfate ratio of 1 exhibited significantly higher residual sulfate concentration compared to CFRs ($P < 0.05$). This finding is consistent with the study reported by Shu et al. [6], which demonstrated that under the COD/sulfate ratio of 1, SBRs exhibited reduced capacity for acclimating CO-SRB compared to CFRs, leading to less efficient sulfate removal due to the lack of CO-SRB to utilize acetate as the electron donor for further sulfate reduction.

3.1.2. Contrasting sulfate reduction and methanogenesis patterns in cycle experiments

The dynamics of sulfate, sulfide, ethanol, acetate, and methane concentrations within cycle experiments are shown in Fig. 1. Sulfate degradation rates varied depending on the carbon source. In the presence of ethanol, the sulfate degradation rate in $SBR_{C/S=2}$, $SBR_{C/S=1}$, $CFR_{C/S=2}$, and $CFR_{C/S=1}$ was 18.9, 37.2, 44.1, and 56.7 mg/(g VSS-h), respectively. However, following complete conversion of ethanol to acetate, the sulfate degradation rates decreased to 1.9, 6.7, 2.5, and 10.8 mg/(g VSS-h), respectively. At the end of the cycle, the sulfide concentration reached 557.4 ± 41.6 , 385.7 ± 20.1 , 647.8 ± 28.9 , and 615.4 ± 9.1 mg/L in $SBR_{C/S=2}$, $SBR_{C/S=1}$, $CFR_{C/S=2}$, and $CFR_{C/S=1}$, respectively. Taking into account the measured pH values, the corresponding concentrations of unionized H_2S were calculated to be 53.9 ± 4.0 , 45.9 ± 2.4 , 62.7 ± 2.8 , and 59.6 ± 0.9 mg/L, respectively. Notably, previous studies have reported a 50 % inhibition of CH_4 production in anaerobic reactors when the H_2S concentration exceeds 50 mg/L [4]. Moreover, the ethanol degradation rates were 56.7, 130.1, 113.8, and 157.7 mg COD/(g VSS-h) for $SBR_{C/S=2}$, $SBR_{C/S=1}$, $CFR_{C/S=2}$, and $CFR_{C/S=1}$, respectively.

It's apparent that a decrease in the COD/sulfate ratio enhanced the sulfate and ethanol degradation rates, with CFRs showing higher rates compared to SBRs at the same COD/sulfate ratio. This superior degradation performance may be attributed to the continuous influent feeding in CFRs, which provided a stable environment for microbial growth and substrate utilization [6,26]. Previous studies also support that SRB and EOB can maintain stable activity under sulfide-rich conditions when operated in continuous systems, indicating that CFRs offer favorable conditions for microbial adaptation to long-term H_2S exposure [18,41].

Regarding methanogenesis, the lag phase for methane production in $SBR_{C/S=2}$, $SBR_{C/S=1}$, $CFR_{C/S=2}$, and $CFR_{C/S=1}$ was 5.2, 4.7, 4.0, and 5.2 h, respectively, with corresponding R_{max} of 15.4, 11.8, 10.8, and 3.3 mL/(g VSS-h). These results indicate superior methane production capabilities in SBRs compared to CFRs. However, decreasing the COD/sulfate ratio adversely affected methanogenesis, likely due to increased competition between SRB and methanogens for common electron donors such as acetate and H_2 . This aligns with previous finding showing that a lower COD/sulfate ratio favors SRB activity over methanogenesis [42].

3.2. H_2S effect on activities of functional microorganisms

3.2.1. CFRs enhanced ethanol degradation and EOB tolerance under H_2S stress

The inhibitory effects of varying initial sulfide concentrations ranging from 0 to 3200 mg/L (corresponding to initial H_2S concentration of 0 to 202.6 mg/L, as calculated using Eq. (1)) on the dynamics of sulfate, ethanol, acetate, and methane are illustrated in Fig. S2. Fig. 2 further summarizes the ethanol degradation rates and sulfate reduction rates, dominated by IO-SRB and EOB under different H_2S concentrations, along with their respective IC_{50} values for H_2S . As shown in

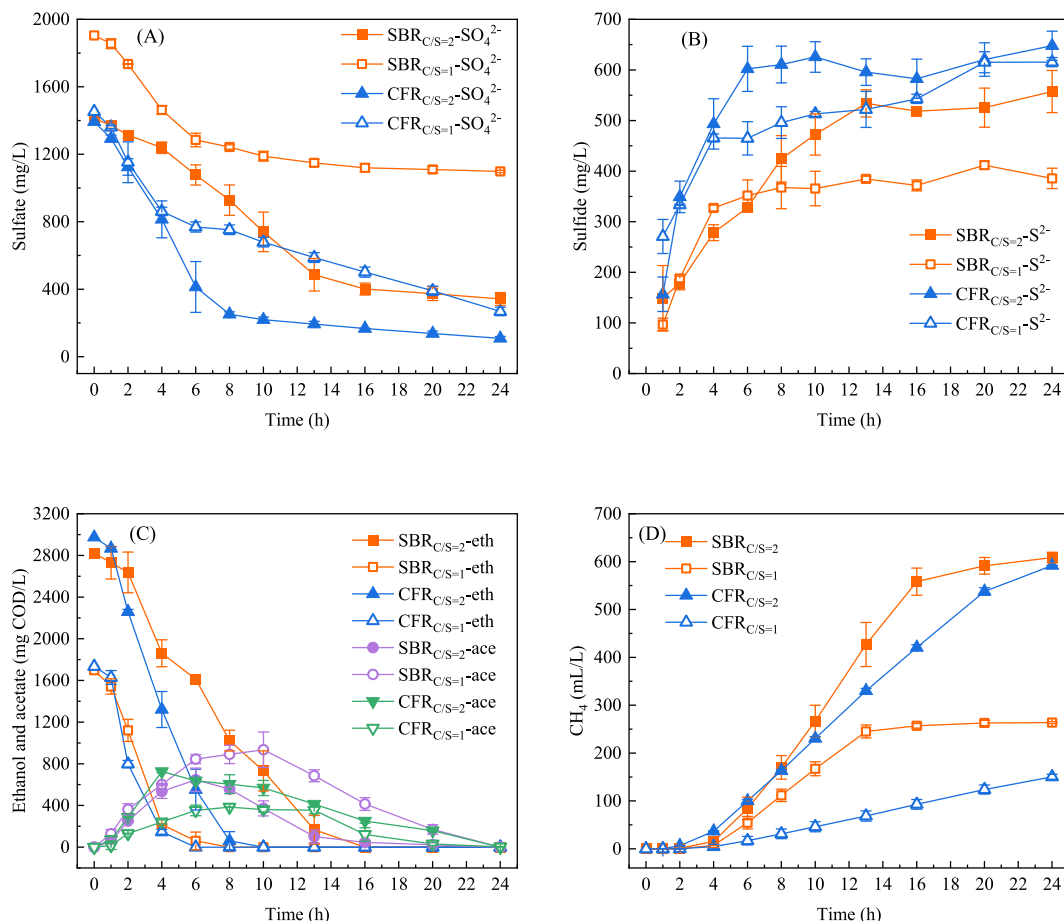


Fig. 1. Dynamics of sulfate (A), sulfide (B), ethanol and acetate (C), and CH_4 (D) in a typical cycle.

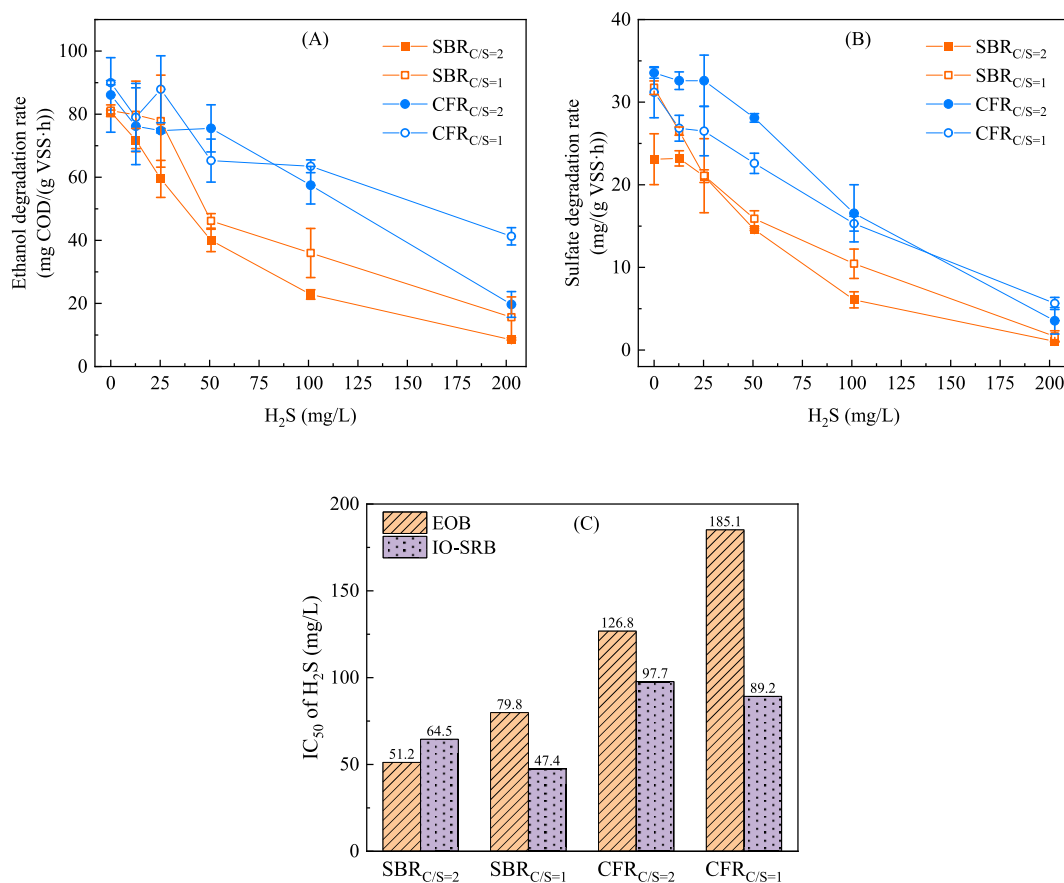


Fig. 2. The effect of H₂S on ethanol (A) and sulfate (B) degradation rate at different H₂S initial concentrations, and the IC₅₀ values of H₂S inhibition for EOB and IO-SRB (C).

Fig. 2A and 2B, ethanol and sulfate degradation rates in CFRs consistently exceeded those in SBRs as H₂S inhibition increased, suggesting that ethanol and sulfate degradation activities in CFRs were less affected by inhibition compared to those in SBRs under the same conditions. Specifically, at an H₂S concentration of 202.6 mg/L, ethanol degradation rate in SBR_{C/S=2}, SBR_{C/S=1}, CFR_{C/S=2}, and CFR_{C/S=1} was inhibited by 89.5 %, 80.7 %, 77.1 %, and 54.1 %, respectively, compared to their rates at 0 mg/L H₂S. Correspondingly, sulfate degradation rate was inhibited by 95.4 %, 94.8 %, 89.4 %, and 81.9 %, respectively. These results indicate that sulfate degradation activity was more severely inhibited than ethanol degradation at high H₂S concentrations ($P < 0.05$). Sulfate reduction involves multiple enzymatic steps and key metal-dependent proteins, such as the Fe-S cluster-containing DsrAB, which are susceptible to inactivation by H₂S binding. In contrast, ethanol degradation involves fewer H₂S-sensitive enzymes, possibly contributing to its greater resilience under H₂S stress [29,43,44].

Fig. 2C summarizes the IC₅₀ values for the activities of EOB and IO-SRB in response to H₂S exposure. Generally, ethanol is primarily utilized by both EOB and IO-SRB. For EOB, the IC₅₀ values were 51.2, 79.8, 126.8, and 185.0 mg/L in SBR_{C/S=2}, SBR_{C/S=1}, CFR_{C/S=2}, and CFR_{C/S=1}, respectively. It is evident that the CFR configuration and the COD/sulfate ratio of 1 promoted greater tolerance of EOB. Additionally, the IC₅₀ value for IO-SRB in SBR_{C/S=2}, SBR_{C/S=1}, CFR_{C/S=2}, and CFR_{C/S=1} was 64.5, 47.4, 97.7, and 89.2 mg/L, respectively. This demonstrates that IO-SRB in CFRs displayed greater tolerance to H₂S inhibition compared to those in SBRs, although lower COD/sulfate ratios tended to reduce IO-SRB tolerance. Overall, except for SBR_{C/S=2}, the IC₅₀ values for EOB were higher than those for IO-SRB in the other three reactors, highlighting the superior resistance of EOB to H₂S inhibition in ethanol degradation [41].

3.2.2. AM showed greater H₂S tolerance than CO-SRB during acetate degradation

To assess acetate degradation under H₂S exposure, batch experiments were conducted with acetate as the sole carbon source and the initial H₂S concentrations ranging from 0 to 202.6 mg/L. The dynamics of sulfate, acetate, and methane concentrations are shown in Fig. S3, and the corresponding degradation rates and IC₅₀ values under H₂S inhibition are summarized in Fig. 3. With increasing H₂S stress, acetate degradation rates in SBRs were generally higher than those in CFRs. A similar phenomenon was observed for R_{max} , with CFR_{C/S=1} showing lower R_{max} values than the other three reactors at all tested H₂S concentrations. However, acetate degradation and CH₄ production were completely inhibited in all reactors at the high H₂S concentrations of 202.6 mg/L. For sulfate degradation rates, SBR_{C/S=1} and CFR_{C/S=1} exhibited higher rates compared to SBR_{C/S=2} and CFR_{C/S=2}. This may be attributed to the lower COD/sulfate ratio, which promotes the enrichment of CO-SRB and facilitates sulfate reduction [6].

The IC₅₀ values for H₂S inhibition of AM and CO-SRB are presented in Fig. 3D. The IC₅₀ value for AM in SBR_{C/S=2}, SBR_{C/S=1}, CFR_{C/S=2}, and CFR_{C/S=1} was 113.2, 75.3, 68.9, and 62.1 mg/L, respectively, with SBR_{C/S=2} demonstrating superior tolerance to H₂S inhibition. Generally, IC₅₀ values in SBRs were higher than those in CFRs, suggesting that methanogenic activity in SBRs was more robust and adaptable to higher H₂S concentrations. However, reducing the COD/sulfate ratio lowered the IC₅₀ values for H₂S in both SBRs and CFRs.

The IC₅₀ value for CO-SRB in SBR_{C/S=2}, SBR_{C/S=1}, CFR_{C/S=2}, and CFR_{C/S=1} was 29.5, 64.7, 25.8, and 39.1 mg/L, respectively, with the highest value observed in SBR_{C/S=1}. In contrast to AM, the COD/sulfate ratio of 1 increased the IC₅₀ values for CO-SRB in both SBRs and CFRs. This inverse relationship may reflect competition between AM and CO-

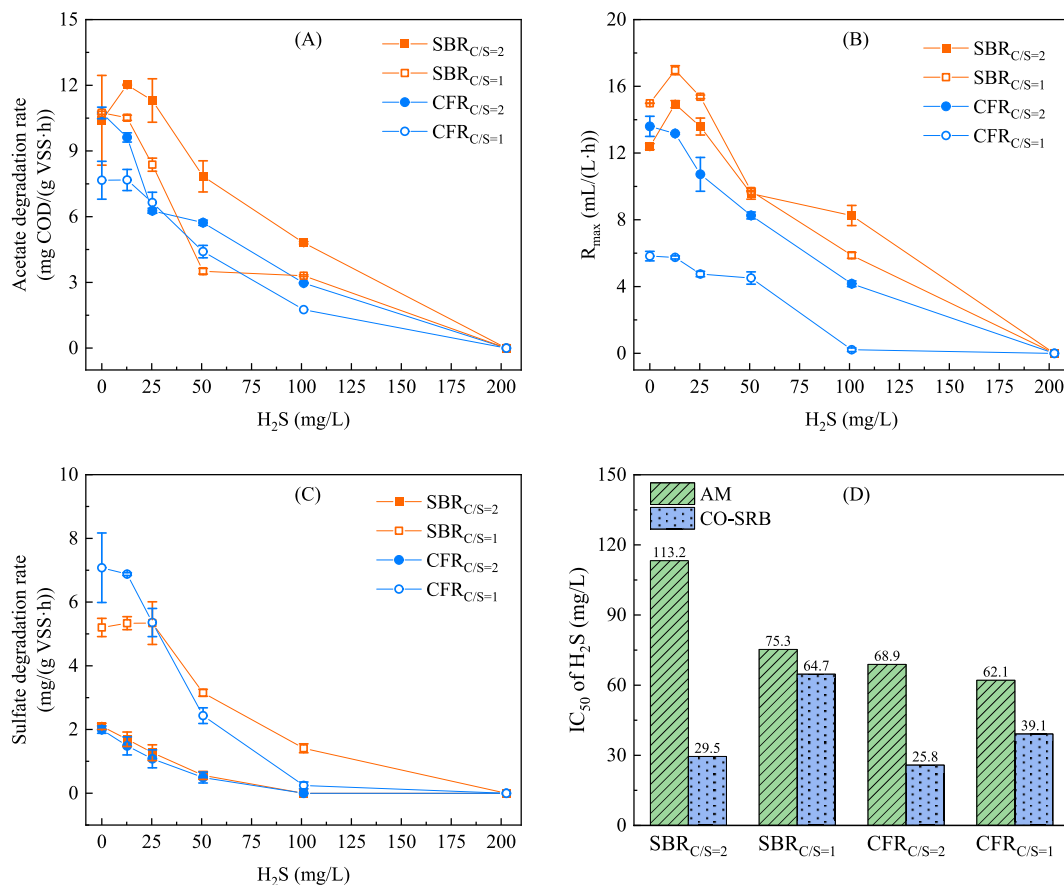


Fig. 3. Effect of H₂S on acetate degradation rate (A), R_{max} (B), and sulfate degradation rate (C) at different H₂S initial concentrations, and the IC₅₀ values of H₂S inhibition for AM and CO-SRB (D).

SRB, as a lower COD/sulfate ratio appears to favor CO-SRB enrichment, potentially reducing AM abundance and thereby decreasing overall AM tolerance to H₂S. Overall, CO-SRB in all four reactors were more sensitive to H₂S inhibition than AM ($P < 0.05$). Maillacheruvu and Parkin [45] also demonstrated that, although CO-SRB exhibit a higher affinity for acetate under substrate-limited conditions, the kinetic and thermodynamic advantages of acetate utilization are offset by their sensitivity to H₂S [13].

3.2.3. HSRB outcompeted HM for H₂ utilization under H₂S stress

To characterize the activity of HM and HSRB under H₂S exposure, degradation experiments were conducted using H₂/CO₂ as the sole substrate source across initial H₂S concentrations ranging from 0 to 202.6 mg/L (Fig. S4 and Fig. 4). The H₂ degradation rate at a high H₂S concentration of 202.6 mg/L was inhibited by 73.9 %, 22.5 %, 13.2 %, and 36.8 % in SBR_{C/S=2}, SBR_{C/S=1}, CFR_{C/S=2}, and CFR_{C/S=1}, respectively. However, methane production was nearly undetectable at this concentration, indicating a strong tolerance of H₂ degradation activity to H₂S inhibition in comparison to methanogenesis, with complete inhibition observed on methanogenesis. The corresponding sulfate degradation rate was inhibited by 86.7 %, 84.3 %, 61.9 %, and 61.1 % in SBR_{C/S=2}, SBR_{C/S=1}, CFR_{C/S=2}, and CFR_{C/S=1}, respectively. These results suggest that H₂ degradation under high H₂S exposure primarily depends on SRB. CFRs were effective in reducing the inhibitory impact of H₂S on sulfate degradation activity when consuming H₂.

In Fig. 4D, the IC₅₀ values for H₂S inhibition were 24.2, 17.5, 48.5, and 89.8 mg/L for HM, and 72.7, 85.5, 195.5, and 156.8 mg/L for HSRB in SBR_{C/S=2}, SBR_{C/S=1}, CFR_{C/S=2}, and CFR_{C/S=1}, respectively. These results indicate that tolerance to H₂S was higher in CFRs than in SBRs for both HM and HSRB. Furthermore, the IC₅₀ values for HSRB consistently

exceeded those for HM, suggesting that HSRB are more resilient to H₂S toxicity. Yamaguchi et al. [46] reported that in a UASB reactor with a COD/sulfate ratio of 2, the IC₅₀ value for HSRB was 380 mg/L, and no HM was detected. This further demonstrates that HSRB can outcompete HM for hydrogen utilization in sulfate-rich environments and exhibits stronger tolerance to H₂S [47].

3.3. Microbial structure and metabolism

3.3.1. Microbial community diverged under different operational mode and H₂S stress

The microbial community result (Fig. 5A) reveals that operational modes and COD/sulfate ratios can selectively enrich species with varying growth strategies and tolerance to H₂S inhibition. For IO-SRB, the relative abundances of *Desulfomicrobium*, *Desulfuromonas*, and *Desulfovibrio* were higher in CFRs than in SBRs. For example, the relative abundance of *Desulfomicrobium* in SBR_{C/S=2}, SBR_{C/S=1}, CFR_{C/S=2}, and CFR_{C/S=1} was 9.3 %, 7.1 %, 12.6 %, and 14.5 %, respectively. These results, along with the high IC₅₀ values for H₂S of IO-SRB in CFRs, suggest that these species exhibit strong tolerance due to continuous high H₂S exposure in CFRs. In particular, both *Desulfomicrobium* and *Desulfovibrio* are capable of utilizing H₂ as an electron donor for sulfate reduction, classifying them as HSRB [48]. In contrast, *Desulfolutivibrio* and *Desulfobulbus* showed higher relative abundances in SBRs compared to CFRs. For instance, *Desulfolutivibrio* had relative abundances of 5.4 %, 8.9 %, 2.4 %, and 4.6 % in SBR_{C/S=2}, SBR_{C/S=1}, CFR_{C/S=2}, and CFR_{C/S=1}, respectively. The fluctuating H₂S exposure in SBRs, where the concentration is lowest at the beginning of each cycle and highest at the end, allows these species to thrive and metabolize rapidly during periods of reduced inhibition [25].

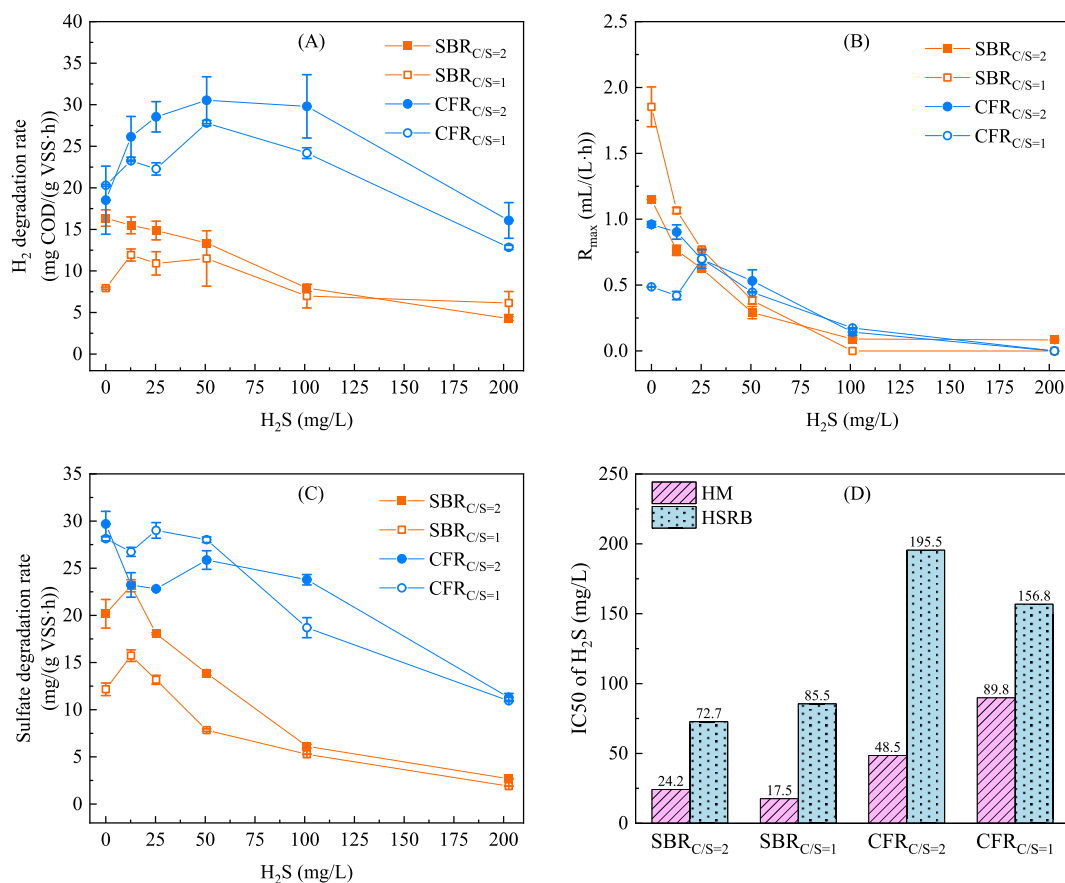


Fig. 4. Effect of H₂S on H₂ degradation rate (A), R_{max} (B), and sulfate degradation rate (C) at different H₂S initial concentrations, and the IC₅₀ values of H₂S inhibition for HM and HSRB (D).

Typical CO-SRB, including *Desulfococcus*, *Desulfobacca*, and *Desulfonema*, demonstrated higher relative abundances in CFRs. For example, *Desulfococcus* showed relative abundance of 3.6 %, 5.4 %, 6.4 %, and 11.2 % in SBR_{C/S=2}, SBR_{C/S=1}, CFR_{C/S=2}, and CFR_{C/S=1}, respectively. *Desulfatitalea* was more abundant in SBRs. Previous studies have suggested that CO-SRB tend to be efficiently enriched in CFRs due to their slow growth rates [6,49]. However, the contrasting distributions of *Desulfococcus*, *Desulfobacca* and *Desulfatitalea* in this study indicate that these CO-SRB genera may have distinct growth kinetics. Oude Elferink et al. [50] reported that *Desulfobacca acetoxidans* has a half-saturation constant for acetate of 0.6 ± 0.4 mM and a μ_{max} of 0.31 1/d to 0.41 1/d. Unfortunately, similar studies on *Desulfatitalea* species are lacking. Thus, this study further demonstrates that different CO-SRB exhibit varying enrichment tendencies depending on reactor configurations. Moreover, these differences highlight that *Desulfobacca* is well-adapted to continuous H₂S exposure, while *Desulfatitalea* is more compatible with the intermittent inhibition of SBRs.

The ethanol-oxidizing *Geobacter*, an important electroactive bacterium, had relative abundances of 3.3 %, 3.3 %, 11.1 %, and 10.6 % in SBR_{C/S=2}, SBR_{C/S=1}, CFR_{C/S=2}, and CFR_{C/S=1}, respectively, indicating that CFRs promoted the enrichment of *Geobacter* [51,52]. The higher IC₅₀ values observed for EOB in CFRs suggest that *Geobacter*, as a dominant member of the EOB group, may have developed resilience to continuous H₂S stress.

The dominant methanogen across the four reactors was the AM *Methanotrix*, with relative abundances of 32.8 %, 19.0 %, 23.9 %, and 13.4 % in SBR_{C/S=2}, SBR_{C/S=1}, CFR_{C/S=2}, and CFR_{C/S=1}, respectively. *Methanotrix* exhibited greater relative abundances in SBRs and under high COD/sulfate ratios [35]. The IC₅₀ values for AM in SBRs were higher than CFRs, suggesting that the intermittent feeding and discharge

provided periods of relief from H₂S inhibition. This cyclical exposure allowed *Methanotrix* to recover during the low-sulfide phase. The relative abundance of *Methanotrix* at the COD/sulfate ratio of 1 were lower compared to that at the ratio of 2, showing CO-SRB are more competitive than AM at lower COD/sulfate ratios [6]. Moreover, *Methanosarcina* and *Methanobacterium*, both belonging to HM, were rarely enriched in the four reactors, with their relative abundance remaining below 0.5 %. This is consistent with the fact that HSRB are more efficient at utilizing H₂ than HM when excessive sulfate is present [50,53]. As a result, it might indicate that the relative abundance and H₂S tolerance of HM is lower than those of HSRB.

Overall, the observed distribution patterns of different microbial groups under varying operational modes and H₂S stress reflect microbial growth strategies. IO-SRB and EOB exhibited higher H₂S tolerance and were preferentially enriched in CFRs with constant H₂S exposure, while AM showed greater sensitivity but demonstrated recovery under dynamic H₂S exposure of SBRs. Moreover, even within the same category (e.g., CO-SRB), genera such as *Desulfobacca* and *Desulfatitalea* displayed contrasting enrichment trends, likely due to their different specific growth kinetics and H₂S sensitivities. These findings highlight that H₂S inhibition does not exert uniform effects across microbial groups, but rather interacts with physiological traits such as growth rate and substrate affinity.

3.3.2. Operational mode shaped microbial metabolic pathways

The analysis of metabolic pathways revealed distinct functional roles and relative abundance of genes associated with microbial communities under different reactor configurations. Key genes involved in sulfate, ethanol, and acetate metabolism were identified and analyzed for their relative abundances (Fig. 5).

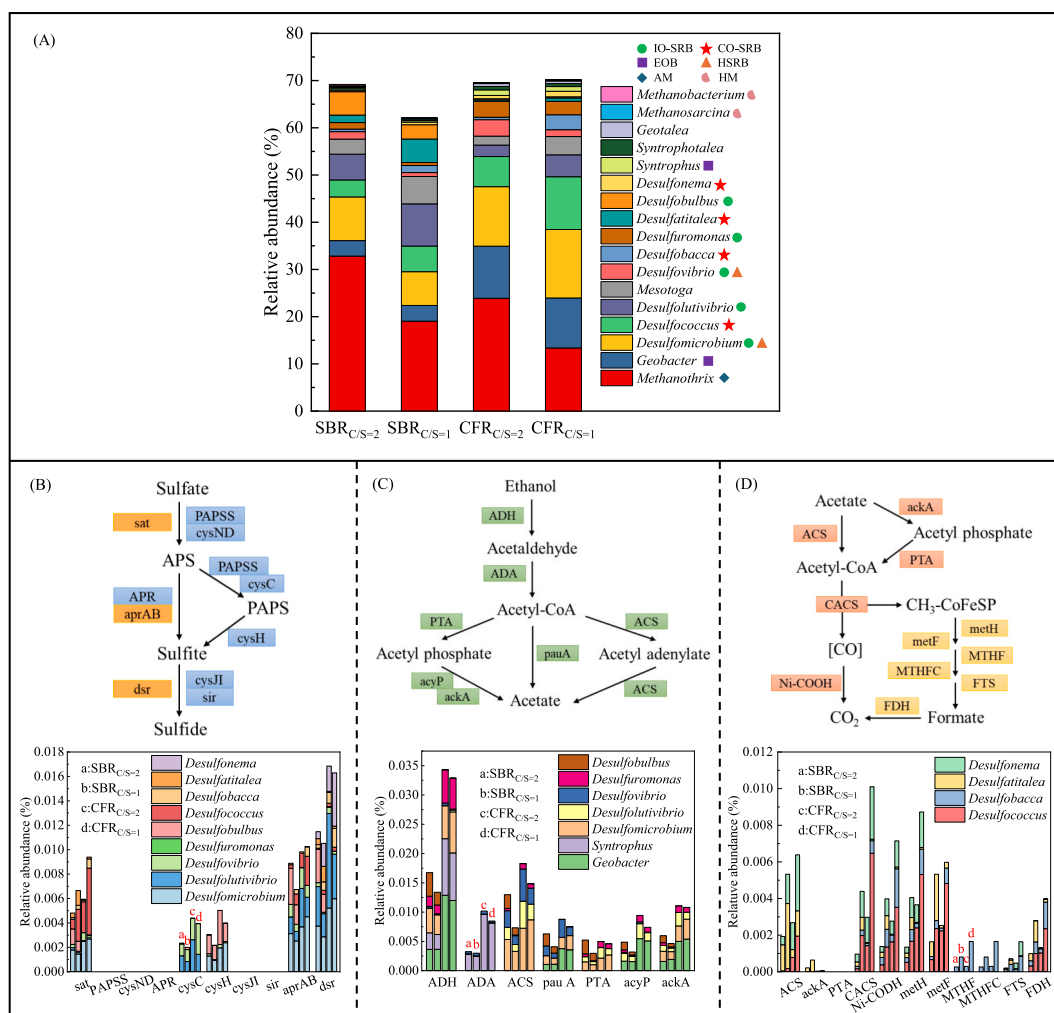


Fig. 5. Microbial community structure at the genus level (A); sulfate metabolic pathway and the relative abundance of functional genes encoding sulfate metabolism pathways in key SRBs (B), the yellow boxes represent enzymes in the DSR pathway, while blue boxes represent enzymes in the ASR pathway; ethanol metabolic pathway and the relative abundances of functional enzymes in functional bacteria encoding ethanol metabolism (C); as well as acetate metabolic pathway and the relative abundances of functional enzymes in functional CO-SRB encoding acetate metabolism (D), the orange boxes represent enzymes in the carbon monoxide dehydrogenase pathway, while yellow boxes represent enzymes in the reverse Wood-Ljungdahl pathway. (For interpretation of the references to colour in this figure legend, the reader is referred to the web version of this article.)

Sulfate metabolism can be categorized into dissimilatory and assimilatory sulfate reduction pathways [54]. As shown in Fig. 5B, most IO-SRB and CO-SRB primarily carried out sulfate metabolism via the dissimilatory pathway, encoded by the genes *sat*, *aprAB*, and *dsr* [55]. The relative abundances of these genes were higher in CFRs compared to those in SBRs, consistent with the enhanced sulfate removal observed in CFRs. This suggests that continuous feeding in CFRs supports more active sulfate reduction. Additionally, the *dsr* genes, involved in the sulfite reduction step, played a crucial role, underscoring the importance of this step in the sequential reduction of sulfate to sulfide within these microbial communities [56].

Ethanol conversion to acetate was facilitated through a series of enzymatic reactions involving *ADH*, *ADA*, *ACS*, and *pauA* (Fig. 5C). Among these, *ADH* plays a critical role in the initial oxidation of ethanol to acetaldehyde, while *ACS* and *pauA* catalyze the subsequent conversion to acetyl-CoA, which enters downstream metabolic pathways. The relative abundances of these genes were consistently higher in CFRs than in SBRs, with the major contributors identified as *Geobacter*, *Syntrophus*, and *Desulfomicrobium*, aligning with their elevated relative abundances [52].

Acetate utilization was predominantly mediated by AM and CO-SRB. The methanogenesis genes were not explicitly analyzed here, as most of

them were attributed to *Methanotrix*. Among CO-SRB, *Desulfococcus*, *Desulfobacca*, *Desulfatitalea*, and *Desulfonema* were the main contributors to acetate oxidation (Fig. 5D). The acetate metabolism pathway driven by CO-SRB involves the conversion of acetate to acetyl-CoA and further intermediates. In particular, the key gene *CACS* catalyzes the conversion of acetyl-CoA to carbon monoxide and methyl cation ($\text{CH}_3\text{-CoFeSP}$), which then enter the carbon monoxide dehydrogenase pathway and the reverse Wood-Ljungdahl pathway [57,58]. The relative abundances of these genes were higher in CFRs, especially at a COD/sulfate ratio of 1, which is consistent with the high complete sulfate reduction rates observed during the cycle experiments.

3.4. Detoxification mechanisms

Under the inhibitory pressure of H_2S , the microbial community in AD systems exhibits a range of biochemical adaptations to sustain normal metabolic activities. Fig. 6 details the differential expression of four key enzyme categories across various microbial groups, including electron transport enzymes, protein repair and regulatory enzymes, specific H_2S metabolic enzymes, and antioxidant defense enzymes. The data reveal that SBRs and CFRs notably impact the enzymatic expression profiles of microbial community, shaping detoxification pathways and survival

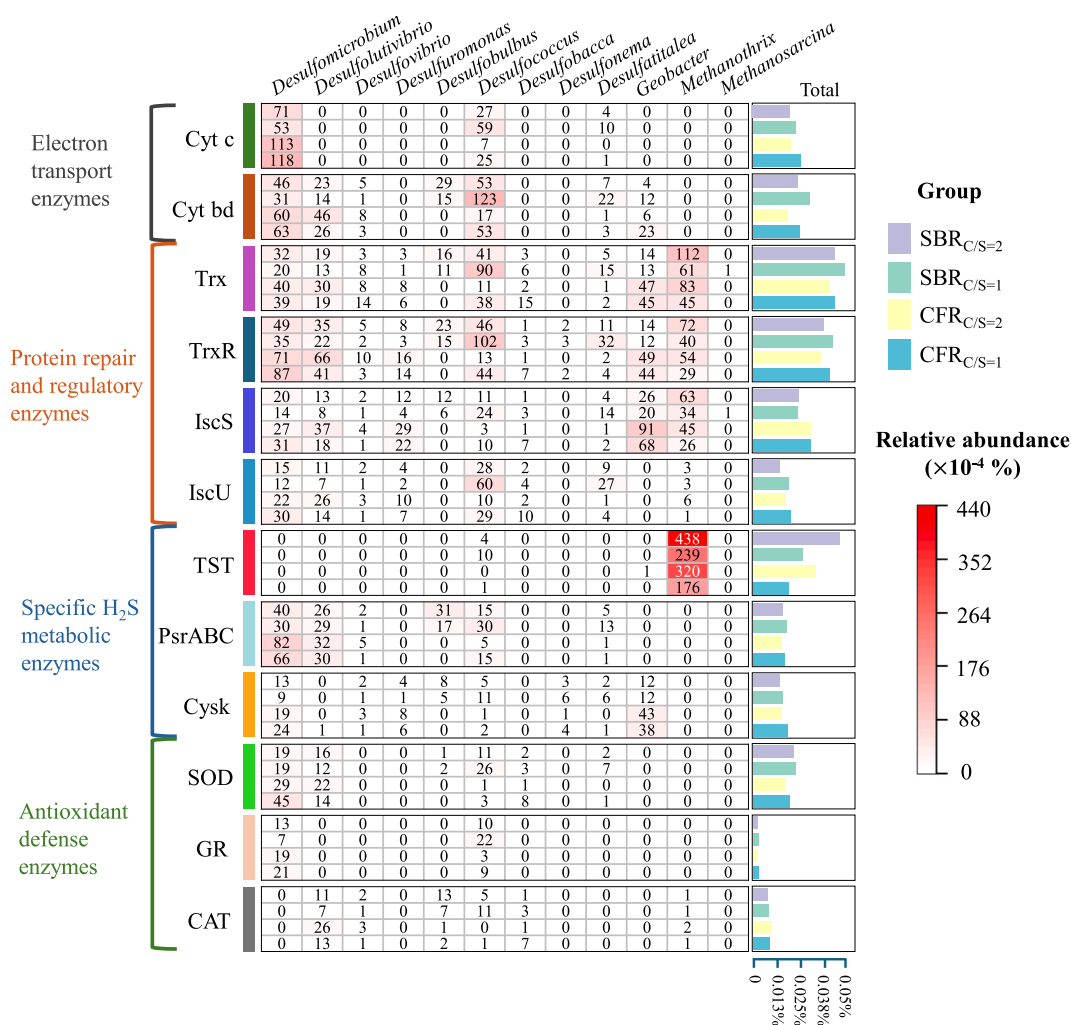


Fig. 6. Differential in the relative abundance of genes encoding enzyme categories across microbial communities under H₂S stress. The data are grouped into four categories: electron transport enzymes, protein repair and regulatory enzymes, specific H₂S metabolic enzymes, and antioxidant defense enzymes. The heatmap illustrates the abundance levels of enzyme genes, with higher abundance represented by darker red shades. The bar charts on the right summarize the total abundance of enzyme categories under different conditions. (For interpretation of the references to colour in this figure legend, the reader is referred to the web version of this article.)

strategies.

In response to H₂S, certain electron transport enzymes such as cytochrome *c* (*cyt c*) and cytochrome *bd* (*cyt bd*) play crucial roles in maintaining electron flow under inhibitory conditions [59]. *Cyt c*, a key electron carrier in the electron transport chain, was highly expressed in *Desulfomicrobium* and *Desulfococcus*. This result suggests that these SRB utilize *cyt c* to enhance electron transfer efficiency, potentially compensating for H₂S-induced disruptions in the electron transport chain [60]. The absence of *cyt c* gene abundance in *Geobacter* and *Methanotherrix* indicates their strategy of shutting down the *cyt c* pathway in response to H₂S pressure. Another essential cytochrome, *cyt bd*, was expressed in various SRB and *Geobacter*. *Cyt bd* has been shown to possess high tolerance to H₂S and can function as an alternative terminal oxidase in H₂S-rich environments [61,62,63]. The expression of *cyt bd* highlights a critical adaptation mechanism in both SRB and *Geobacter*, enabling them to perform respiration and survival in H₂S-rich conditions.

The data highlights a marked increase in thioredoxin (*trx*), thioredoxin reductase (*trxR*), cysteine desulfurase (*iscS*), and iron-sulfur cluster assembly scaffold protein (*iscU*) across most microbial communities, emphasizing the universal need for protein repair under H₂S stress [29,64]. H₂S has been reported to disrupt protein structures by reducing disulfide bonds or disrupting Fe-S clusters by binding to iron

atoms [65]. Elevated levels of *trx*, *trxR*, *iscS*, and *iscU* indicate an active defense mechanism to mitigate protein oxidation and restore functional conformations. The upregulation of these enzymes in SRB, *Geobacter*, and *Methanotherrix* points to a critical repair pathway that offsets the destabilizing effects of H₂S on cellular proteins.

One of the most distinctive detoxification strategies observed was the selective expression of specific H₂S metabolic enzymes [66,67]. TST is a crucial enzyme in the H₂S oxidation route that leads to the formation of hydropersulfides, thiosulfate and sulfate [31,68]. Only *Methanotherrix* showed the highest relative gene abundance for TST, suggesting a unique pathway for converting H₂S into less toxic sulfur compounds. Additionally, both IO-SRB and CO-SRB exhibited higher gene abundance for polysulfide reductase (*psr ABC*) [69,70]. This enzyme complex likely helps these bacteria convert toxic polysulfides into less harmful compounds, thereby enhancing their survival in high H₂S environments. The expression of cysteine synthase (*cysK*) in *Geobacter* under H₂S stress underscores a crucial detoxification mechanism where H₂S is directly incorporated into metabolic pathways. *CysK* catalyzes the synthesis of cysteine by utilizing H₂S as a sulfur donor, effectively reducing H₂S levels in the environment. This process not only detoxifies H₂S but also produces cysteine, a vital precursor for iron-sulfur (Fe-S) cluster synthesis and cellular redox balance [31]. The upregulation of *cysK* in *Geobacter* suggests that this microorganism employs cysteine

biosynthesis as a strategy to mitigate H₂S toxicity while supporting the repair and stabilization of Fe-S clusters essential for electron transport chain function.

Interestingly, antioxidant defense enzymes such as superoxide dismutase (SOD), glutathione reductase (GR), and catalase (CAT) were minimally expressed in SRB and absent in *Geobacter* and *Methanotrix*, implying a nuanced response to oxidative stress in H₂S-rich environments [33,71]. The low-level expression of these enzymes in SBR suggests a baseline antioxidant defense sufficient for managing minor oxidative stress, without heavily relying on reactive oxygen species (ROS) detoxification pathways. This may be because SRB typically operates under strict anaerobic conditions where ROS generation is inherently low. However, the presence of SOD and CAT, even at low levels, indicates a preparedness to manage transient oxidative events, possibly induced by electron leakage from H₂S [27]. Conversely, the absence of these enzymes in *Geobacter* and *Methanotrix* suggests that these microbes rely on non-oxidative mechanisms, such as direct H₂S detoxification pathways (e.g., *cysK* in *Geobacter* and TST in *Methanotrix*), rather than ROS-based defense mechanisms.

In conclusion, microorganisms adopt distinct detoxification and survival strategies under H₂S stress, which are affected by the operational modes. The CFRs mode fostered the growth of H₂S-tolerant species like *Geobacter* and *Desulfomicrobium*, substantially enhancing ethanol degradation under H₂S pressure. This suggests that CFRs may support a microbial community structure that relies on non-traditional detoxification mechanisms, such as increased cysteine biosynthesis via *cysK* and sulfur cycling via *psrABC*, to resist H₂S inhibition. Compared to CFRs, SBRs led to higher relative abundance of *Methanotrix*, which leveraged TST for direct H₂S detoxification, facilitating methanogenesis. The high abundance of TST in *Methanotrix* may be crucial for methanogens to overcome H₂S toxicity by transforming it into less harmful sulfur species, thereby enhancing methanogenic activity in SBRs. Therefore, incorporating CFRs in scenarios where sulfate reduction is the primary treatment mechanism (or when lower COD/sulfate ratios are present) can enhance microbial detoxification. CFRs facilitate the continuous exchange of substrates and microbial adaptation to sulfate and H₂S stresses, making them ideal for treating high-sulfate wastewater. Conversely, for systems where methane production is a key goal (or when higher COD/sulfate ratios are involved), SBRs with periodic feeding, reaction, and settling cycles can encourage the growth of methanogens that help reduce the impact of H₂S.

4. Conclusion

This study provides insights into microbial responses to H₂S stress in AD systems under different reactor configurations and COD/sulfate ratios. CFRs with the COD/sulfate ratio of 1 enhanced sulfate reduction and ethanol degradation under H₂S stress, while SBRs with the COD/sulfate ratio of 2 supported higher methanogenic activity. EOB, IO-SRB, HSRB, and HM exhibited higher H₂S tolerance in CFRs, while AM and CO-SRB showed greater tolerance in SBRs. SBRs facilitated *Methanotrix* enrichment and its unique detoxification mechanism via TST abundance. Conversely, *Desulfomicrobium* and *Geobacter* were enriched in CFRs, mitigating H₂S inhibition through increased *cyt bd* and *cysK*, respectively.

CRediT authorship contribution statement

Wenhui Shu: Writing – original draft, Methodology, Investigation, Formal analysis. **Bang Du:** Writing – review & editing, Methodology, Formal analysis. **Guangxue Wu:** Writing – review & editing, Supervision, Funding acquisition, Conceptualization.

Declaration of competing interest

The authors declare the following financial interests/personal

relationships which may be considered as potential competing interests: Guangxue Wu reports financial support was provided by Science Foundation Ireland. Guangxue Wu reports financial support was provided by Sustainable Energy Authority of Ireland. Wenhui Shu reports financial support was provided by China Scholarship Council. If there are other authors, they declare that they have no known competing financial interests or personal relationships that could have appeared to influence the work reported in this paper.

Acknowledgements

This study was supported by the Taighde Éireann – Research Ireland (formerly Science Foundation Ireland) and the Sustainable Energy Authority of Ireland under the SFI Frontiers for the Future Awards Programme (22/FFP-A/10346). Wenhui Shu thanks the scholarship from the China Scholarship Council (No: 202106790006). Guangxue Wu thanks for the support from the Galway University Foundation.

Appendix A. Supplementary data

Supplementary data to this article can be found online at <https://doi.org/10.1016/j.cej.2025.162766>.

Data availability

Data will be made available on request.

References

- [1] P. Garkoti, J.Q. Ni, S.K. Thengane, Energy management for maintaining anaerobic digestion temperature in biogas plants, *Renew. Sustain. Energy Rev.* 199 (2024) 114430.
- [2] P.M. Subbarao, T.C. D'Silva, K. Adlak, S. Kumar, R. Chandra, V.K. Vijay, Anaerobic digestion as a sustainable technology for efficiently utilizing biomass in the context of carbon neutrality and circular economy, *Environ. Res.* 234 (2023) 116286.
- [3] T. Meyer, E.A. Edwards, Anaerobic digestion of pulp and paper mill wastewater and sludge, *Water Res.* 65 (2014) 321–349.
- [4] W. Li, Q. Niu, H. Zhang, Z. Tian, Y. Zhang, Y. Gao, Y.-Y. Li, O. Nishimura, M. Yang, UASB treatment of chemical synthesis-based pharmaceutical wastewater containing rich organic sulfur compounds and sulfate and associated microbial characteristics, *Chem. Eng. J.* 260 (2015) 55–63.
- [5] Q. Huang, Y. Liu, B.R. Dhar, Deciphering the microbial interactions and metabolic shifts at different COD/sulfate ratios in electro-assisted anaerobic digestion, *J. Hazard. Mater.* 480 (2024) 135801.
- [6] W. Shu, B. Du, G. Wu, Strategies for enriching targeted sulfate-reducing bacteria and revealing their microbial interactions in anaerobic digestion ecosystems, *Water Res.* 270 (2025) 122842.
- [7] P. Nicholls, D.C. Marshall, C.E. Cooper, M.T. Wilson, Sulfide inhibition of and metabolism by cytochrome c oxidase, *Biochem Soc Trans.* 41 (5) (2013) 1312–1316.
- [8] C. Felbek, F. Arrigoni, D. de Sancho, A. Jacq-Bailly, R.B. Best, V. Fourmond, L. Bertini, C. Léger, Mechanism of hydrogen sulfide-dependent inhibition of FeFe hydrogenase, *ACS Catal.* 11 (24) (2021) 15162–15176.
- [9] X. Dai, C. Hu, D. Zhang, Y. Chen, A new method for the simultaneous enhancement of methane yield and reduction of hydrogen sulfide production in the anaerobic digestion of waste activated sludge, *Bioresour. Technol.* 243 (2017) 914–921.
- [10] H.-Z. Wang, J. Li, Y. Yi, M.K. Nobu, T. Narihiro, Y.-Q. Tang, Response to inhibitory conditions of acetate-degrading methanogenic microbial community, *J. Biosci. Bioeng.* 129 (4) (2020) 476–485.
- [11] L. Krayzelova, J. Bartacek, I. Diaz, D. Jeison, E.I.P. Volcke, P. Jenicek, Microaeration for hydrogen sulfide removal during anaerobic treatment: a review, *Rev. Environ. Sci. Bio/technol.* 14 (2015) 703–725.
- [12] C.M. Dykstra, S.G. Pavlostathis, Hydrogen sulfide affects the performance of a methanogenic bioelectrochemical system used for biogas upgrading, *Water Res.* 200 (2021) 117268.
- [13] J. Lee, S. Hwang, Single and combined inhibition of *Methanosaeta concilii* by ammonia, sodium ion and hydrogen sulfide, *Bioresour. Technol.* 281 (2019) 401–411.
- [14] H.P. Vu, L.N. Nguyen, Q. Wang, H.H. Ngo, Q. Liu, X. Zhang, L.D. Nghiem, Hydrogen sulphide management in anaerobic digestion: a critical review on input control, process regulation, and post-treatment, *Bioresour. Technol.* 346 (2022) 126634.
- [15] Y. Wang, Q. Fu, F. Yang, X. Li, X. Ma, Y. Xu, X. Liu, D. Wang, Mechanistic insights into Fe₃O₄-mediated inhibition of H₂S gas production in sludge anaerobic digestion, *Water Res.* 267 (2024) 122464.

- [16] H. Yuan, N. Zhu, Progress in inhibition mechanisms and process control of intermediates and by-products in sewage sludge anaerobic digestion, *Renew. Sustain. Energy Rev.* 58 (2016) 429–438.
- [17] V. O'Flaherty, T. Mahony, R. O'Kennedy, E. Colleran, Effect of pH on growth kinetics and sulphide toxicity thresholds of a range of methanogenic, syntrophic and sulphate-reducing bacteria, *Process Biochem.* 33 (5) (1998) 555–569.
- [18] S. Okabe, P.H. Nielsen, W.L. Jones, W.G. Characklis, Sulfide product inhibition of *Desulfivobrio desulfuricans* in batch and continuous cultures, *Water Res.* 29 (2) (1995) 571–578.
- [19] B. Igen, S. Harrison, Exposure to sulfide causes populations shifts in sulfate-reducing consortia, *Res. Microbiol.* 157 (8) (2006) 784–791.
- [20] Z. Wang, S. Wang, Y. Hu, B. Du, J. Meng, G. Wu, H. Liu, X. Zhan, Distinguishing responses of acetoclastic and hydrogenotrophic methanogens to ammonia stress in mesophilic mixed cultures, *Water Res.* 224 (2022) 119029.
- [21] N. Paepating, N. Boonapatcharoen, W. Songkasiri, H. Yasui, C. Phalakornkule, Recovery of anaerobic system treating sulfate-rich wastewater using zero-valent iron, *Chem. Eng. J.* 435 (2022) 135175.
- [22] B. Demirel, P. Scherer, The roles of acetotrophic and hydrogenotrophic methanogens during anaerobic conversion of biomass to methane: a review, *Rev. Environ. Sci. Bio/technol.* 7 (2008) 173–190.
- [23] M. Andreides, L. Pokorná-Krayzelová, J. Bartáček, J. Bartáček, Stirring-based control strategy for microaerobic H₂S removal in sequencing batch anaerobic digesters, *Fuel* 306 (2021) 121696.
- [24] J.J. González-Cortés, S. Torres-Herrera, F. Almenglo, M. Ramírez, D. Cantero, Anoxic biogas biodesulfurization promoting elemental sulfur production in a Continuous Stirred Tank Bioreactor, *J. Hazard. Mater.* 401 (2021) 123785.
- [25] M. Sekine, S. Akizuki, M. Kishi, T. Toda, Stable nitrification under sulfide supply in a sequencing batch reactor with a long fill period, *J. Water Process. Eng.* 25 (2018) 190–194.
- [26] Q. Guo, Q. Yin, J. Du, J. Zuo, G. Wu, New insights into the r/K selection theory applied in methanogenic systems through continuous-flow and sequencing batch operational modes, *Sci. Total Environ.* 807 (2022) 150732.
- [27] B. Zhang, J. Liu, C. Cai, Y. Zhou, Harnessing high-level hydrogen sulfide stress for enhanced biogas utilization: Adaptive resilience of a mixed-culture system, *Chem. Eng. J.* 506 (2025) 160300.
- [28] T. Shimizu, S. Masuda, Persulfide-responsive transcriptional regulation and metabolism in bacteria, *J. Biochem.* 167 (2) (2020) 125–132.
- [29] S. Han, Y. Li, H. Gao, Generation and physiology of hydrogen sulfide and reactive sulfur species in bacteria, *Antioxidants* 11 (12) (2022) 2487.
- [30] S. Ramasamy, S. Singh, P. Taniere, M.J.S. Langman, M.C. Eggo, Sulfide-detoxifying enzymes in the human colon are decreased in cancer and upregulated in differentiation, *Am J Physiol Gastrointest Liver Physiol.* 291 (2) (2006) G288–G296.
- [31] G. Ghiotto, N. De Bernardini, G. Giangeri, P. Tsapekos, M. Gaspari, P.G. Kougias, S. Campanaro, I. Angelidaki, L. Treu, From microbial heterogeneity to evolutionary insights: a strain-resolved metagenomic study of H₂S-induced changes in anaerobic biofilms, *Chem. Eng. J.* 485 (2024) 149824.
- [32] S. Korshunov, K.R.C. Imlay, J.A. Imlay, The cytochrome *bd* oxidase of *Escherichia coli* prevents respiratory inhibition by endogenous and exogenous hydrogen sulfide, *Mol. Microbiol.* 101 (1) (2016) 62–77.
- [33] C. Kaya, M. Ashraf, Sodium hydrosulfite together with silicon detoxifies arsenic toxicity in tomato plants by modulating the AsA-GSH cycle, *Environ. Pollut.* 294 (2022) 118608.
- [34] J. Shen, H. Peng, Y. Zhang, J.C. Trinidad, D.P. Giedroc, *Staphylococcus aureus* *sqr* encodes a type II sulfide: quinone oxidoreductase and impacts reactive sulfur speciation in cells, *Biochemistry* 55 (47) (2016) 6524–6534.
- [35] J. Du, X. Zhou, Q. Yin, J. Zuo, G. Wu, Revealing impacts of operational modes on anaerobic digestion systems coupling with sulfate reduction, *Bioresour. Technol.* 385 (2023) 129431.
- [36] R.-C. Jin, G.-F. Yang, Q.-Q. Zhang, C. Ma, J.-J. Yu, B.-S. Xing, The effect of sulfide inhibition on the ANAMMOX process, *Water Res.* 47 (3) (2013) 1459–1469.
- [37] APHA, Standard methods for the examination of water and wastewater, 21st ed., American Public Health Association, American Water Works Association, Water Environment Federation, Washington DC, 2005.
- [38] M.H. Zwietering, I. Jongenburger, F.M. Rombouts, Modeling of the bacterial growth curve, *Appl. Environ. Microbiol.* 56 (6) (1990) 1875–1881.
- [39] B. Niu, Y. Xie, H. Sun, X. Zhou, Removal behavior, inhibition kinetics, microbial community and metabolic pathways in simultaneous anammox and denitrification under indole exposure, *J. Environ. Chem. Eng.* 12 (2) (2024) 112296.
- [40] M. Kanehisa, S. Goto, KEGG: kyoto encyclopedia of genes and genomes, *Nucleic Acids Res.* 28 (1) (2000) 27–30.
- [41] V. Uberoi, S.K. Bhattacharya, Interactions among sulfate reducers, acetogens, and methanogens in anaerobic propionate systems, *Water Environ. Res.* 67 (3) (1995) 330–339.
- [42] C. O'Reilly, E. Colleran, Effect of influent COD/SO₄²⁻ ratios on mesophilic anaerobic reactor biomass populations: physico-chemical and microbiological properties, *FEMS Microbiol. Ecol.* 56 (1) (2006) 141–153.
- [43] C. Kämpel, M. Grosser, T.S. Tanabe, C. Dahl, Fe/S proteins in microbial sulfur oxidation, *Biochim. Biophys. Acta - Mol. Cell Res.* 1871 (5) (2024) 119732.
- [44] T.M. Mwene-Mbeja, A. Dufour, J. Lecka, B.S. Kaur, C. Vaneeckhaute, Enzymatic reactions in the production of biomethane from organic waste, *Enzyme Microb. Technol.* 132 (2020) 109410.
- [45] K.Y. Maillacheruvu, G.F. Parkin, Kinetics of growth, substrate utilization and sulfide toxicity for propionate, acetate, and hydrogen utilizers in anaerobic systems, *Water Environ. Res.* 68 (7) (1996) 1099–1106.
- [46] T. Yamaguchi, H. Harada, T. Hisano, S. Yamazaki, I.-C. Tseng, Process behavior of UASB reactor treating a wastewater containing high strength sulfate, *Water Res.* 33 (14) (1999) 3182–3190.
- [47] S. Pender, M. Toomey, M. Carton, D. Eardly, J.W. Patching, E. Colleran, V. O'Flaherty, Long-term effects of operating temperature and sulphate addition on the methanogenic community structure of anaerobic hybrid reactors, *Water Res.* 38 (3) (2004) 619–630.
- [48] E. Rodríguez, A. Lopes, M. Fdz.-Polanco, A.J. Stams, P.A. García-Encina, Molecular analysis of the biomass of a fluidized bed reactor treating synthetic vinasse at anaerobic and micro-aerobic conditions, *Appl. Microbiol. Biotechnol.* 93 (2012) 2181–2191.
- [49] P. Schönheit, J.K. Kristjansson, R.K. Thauer, Kinetic mechanism for the ability of sulfate reducers to out-compete methanogens for acetate, *Arch. Microbiol.* 132 (1982) 285–288.
- [50] S.J.W.H. Oude Elferink, A. Visser, L.W. Hulshoff Pol, A.J.M. Stams, Sulfate reduction in methanogenic bioreactors, *FEMS Microbiol. Rev.* 15 (2–3) (1994) 119–136.
- [51] A.-E. Rotaru, P.M. Shrestha, F. Liu, B. Markovaite, S. Chen, K.P. Nevin, D.R. Lovley, Direct interspecies electron transfer between *Geobacter metallireducens* and *Methanosarcina barkeri*, *Appl. Environ. Microbiol.* 80 (15) (2014) 4599–4605.
- [52] B. Du, X. Zhan, P.N. Lens, Y. Zhang, G. Wu, Deciphering anaerobic ethanol metabolic pathways shaped by operational modes, *Water Res.* 249 (2024) 120896.
- [53] S.A. Dar, R. Kleerebezem, A.J.M. Stams, J.G. Kuenen, G. Muyzer, Competition and coexistence of sulfate-reducing bacteria, acetogens and methanogens in a lab-scale anaerobic bioreactor as affected by changing substrate to sulfate ratio, *Appl. Microbiol. Biotechnol.* 78 (2008) 1045–1055.
- [54] Z. Zhou, P.Q. Tran, E.S. Cowley, E. Trembath-Reichert, K. Anantharaman, Diversity and ecology of microbial sulfur metabolism, *Nat. Rev. Microbiol.* 23 (2024) 122–140.
- [55] J. Li, Y. Feng, D. Wang, Y. Li, M. Cai, Y. Tian, Y. Pan, X. Chen, Q. Zhang, A. Li, Optimization of sulfate reduction and methanogenesis via phase separation in a two-phase internal circulation reactor for the treatment of high-sulfate organic wastewater, *Water Res.* 260 (2024) 121918.
- [56] S. Neukirchen, I.A.C. Pereira, F.L. Sousa, Stepwise pathway for early evolutionary assembly of dissimilatory sulfite and sulfate reduction, *ISME J.* 17 (10) (2023) 1680–1692.
- [57] D. Goevart, R. Conrad, Carbon isotope fractionation by sulfate-reducing bacteria using different pathways for the oxidation of acetate, *Environ. Sci. Technol.* 42 (21) (2008) 7813–7817.
- [58] T. Svetlichnaia, V. Svetlichnyi, O. Meyer, H. Dobbek, Structural insights into methyltransfer reactions of a corrinoid iron-sulfur protein involved in acetyl-CoA synthesis, *Proc. Natl. Acad. Sci. USA* 103 (39) (2006) 14331–14336.
- [59] M.R. Nastasi, L. Caruso, F. Giordano, M. Mellini, G. Rampioni, A. Giuffrè, E. Forte, Cyanide insensitive oxidase confers hydrogen sulfide and nitric oxide tolerance to *Pseudomonas aeruginosa* aerobic respiration, *Antioxidants* 13 (3) (2024) 383.
- [60] V. Vitvitsky, J.L. Miljkovic, T. Bostelaar, B. Adhikari, P.K. Yadav, A.K. Steiger, R. Torregrossa, M.D. Pluth, M. Whiteman, R. Banerjee, M.R. Filipovic, Cytochrome *c* reduction by H₂S potentiates sulfide signaling, *ACS Chem. Biol.* 13 (8) (2018) 2300–2307.
- [61] E. Forte, V.B. Borisov, M. Falabella, H.G. Colaco, M. Tinajero-Trejo, R.K. Poole, J.B. Vicente, P. Sarti, A. Giuffrè, The terminal oxidase cytochrome *bd* promotes sulfide-resistant bacterial respiration and growth, *Sci. Rep.* 6 (1) (2016) 23788.
- [62] V.B. Borisov, E. Forte, Terminal oxidase cytochrome *bd* protects bacteria against hydrogen sulfide toxicity, *Biochem. Mosc.* 86 (2021) 22–32.
- [63] R.A. Schmitz, S.H. Peeters, S.S. Mohammadi, T. Berben, T. van Erven, C.A. Iosif, T. van Alen, W. Versantvoort, M.S.M. Jetten, H.J.M. Op den Camp, A. Pol, Simultaneous sulfide and methane oxidation by an extremophile, *Nat. Commun.* 14 (1) (2023) 2974.
- [64] T. Vignane, M.R. Filipovic, Emerging chemical biology of protein persulfidation, *Antioxid. Redox Signal.* 39 (1–3) (2023) 19–39.
- [65] L. Ryzd, M. Wróbel, H. Jurkowska, Sulfur administration in Fe-S cluster homeostasis, *Antioxidants* 10 (11) (2021) 1738.
- [66] U. Theissen, W. Martin, Sulfide: quinone oxidoreductase (SQR) from the lugworm *Arenicola marina* shows cyanide- and thioredoxin-dependent activity, *FEBS J.* 275 (6) (2008) 1131–1139.
- [67] Y. Sun, M. Wang, Z. Zhong, H. Chen, H. Wang, L. Zhou, L. Cao, L. Fu, H. Zhang, C. Lian, S. Sun, C. Li, Adaptation to hydrogen sulfide-rich environments: Strategies for active detoxification in deep-sea symbiotic mussels, *Gigantidas platifrons*, *Sci. Total Environ.* 804 (2022) 150054.
- [68] S. Buonvino, I. Arciero, S. Melino, Thiosulfate-cyanide sulfurtransferase a mitochondrial essential enzyme: from cell metabolism to the biotechnological applications, *Int. J. Mol. Sci.* 23 (15) (2022) 8452.
- [69] J. Liang, H. Huang, Y. Wang, L. Li, J. Yi, S. Wang, A cytoplasmic NAD (P) H-dependent polysulfide reductase with thiosulfate reductase activity from the hyperthermophilic bacterium *Thermotoga maritima*, *Microbiol. Spectrum.* 10 (4) (2022) e00436–e00522.
- [70] J.J. Wright, K. Mewis, N.W. Hanson, K.M. Konwar, K.R. Maas, S.J. Hallam, Genomic properties of Marine Group A bacteria indicate a role in the marine sulfur cycle, *ISME J.* 8 (2) (2014) 455–468.
- [71] J. Li, X. Ran, M. Zhou, K. Wang, H. Wang, Y. Wang, Oxidative stress and antioxidant mechanisms of obligate anaerobes involved in biological waste treatment processes: a review, *Sci. Total Environ.* 838 (2022) 156454.